AN EXTENSIVE EXPERIMENTAL INVESTIGATION OF SHALLOW- AND CONFINED-WATER EFFECTS ON THE MANOEUVRING FORCES OF A 110M INLAND SHIP

Antoine Bedos and **Roberto Tonelli**, Maritime Research Institute Netherlands (MARIN), The Netherlands

SUMMARY

Due to the complexity of the physics in shallow water and lack of benchmark, more insights are needed to derive accurate mathematical models for time-domain simulations. For this reason, three model test campaigns were performed in different facilities with the 110m MARIN Inland Ship (MISS 110), a representative class-Va inland ship. Experiments were conducted in a captive set-up, at various water depths. All kinds of planar motions were imposed, using a Computerised Planar Motion Carriage (CPMC) technique. In particular, this enabled high-quality measurement during steady rotation motions, which cannot be performed in narrow tanks.
This paper makes experimental data available to the public. It evidences the increase in hull loads for lower under-keel clearances and the effect of blockage on experimental results in conventional tanks. It also shows the non-linearity of hull loads with respect to V_s^2 in very shallow water, and linked it to the squat effect.

NOMENCLATURE

L_{pp}	Length between perpendiculars [m]
T	Mean draught at rest [m]
h/T	Water depth-to-draught ratio [-]
n	Propeller revolution rate [1/min]
F_r	Froude number [-]
ρ	Density of water [1000.0 kg/m^3]
V_s	Ship speed [km/h]
u	Longitudinal speed [m/s]
v	Transversal speed [m/s]
r	Yaw rate [deg/s]
β	Drift angle [deg]
r'	Non-dimensional yaw rate [-]
X	Hull surge force [kN]
Y	Hull sway force [kN]
N	Hull yaw moment [kN·m]
X'	Hull non-dimensional surge force [-]
Y'	Hull non-dimensional sway force [-]
N'	Hull non-dimensional yaw moment [-]

BT	Shallow-Water Basin/Binnenvaart Tank
CFD	Computational fluid dynamics
CPMC	Computerised Planar Motion Carriage
MISS 110	110m MARIN Inland Standard Ship
OB	Offshore Basin
PMM	Planar Motion Mechanism
UKC	Under-keel clearance

1 INTRODUCTION

As a consequence of climate change, European rivers have experienced low-water episodes increasingly over the last years, jeopardizing inland shipping traffic and challenging local safety policies and guidelines. In the Netherlands, this led Dutch ministry of infrastructure and water management (Rijkswaterstaat) and the Maritime Research Institute Netherlands (MARIN) to launch a joint research project on shallow-water effects in 2019. This study aims at developing high-fidelity simulation models to investigate the effect of extreme shallow-water conditions on the manoeuvring performance of inland ships, providing advice and recommendations to shipping and waterway authorities.

Deriving accurate modular models for time-domain simulations requires sufficient understanding of the underlying physics, as well as reliable predictions of manoeuvring loads of the hull and its appendages. However, this proves to be significantly more challenging in shallow water than for deep-water cases. In fact, the flow behaviour around the ship is strongly water-depth dependent, thus deep-water formulations and their assumptions quickly become non-applicable as the under-keel clearance (UKC) decreases. These changing flow characteristics make the loads on the hull and its appendages, as well as their interactions, greatly water-depth dependent. In other words, understanding and quantifying manoeuvring loads at an UCK of 20% and 100% only brings limited knowledge for an UKC of 40%. In addition, hardly any reliable benchmark is available for inland ships. This is partially due to the complexity of deriving such data. Full-scale trials provide valuable insights but they are subject to environmental conditions. Numerical tools using Computational Fluid Dynamics (CFD) techniques enable a controlled environment, but lack validation and are very sensitive to numerical settings and turbulence models, especially in very shallow water. Finally, scaled model tests require specific facilities, as restricted tank widths introduce undesirable phenomena such as blockage (Raven, 2019a, 2019b; Mucha et al, 2019).

Due to the complexity of the underlying physics and lack of reliable benchmark, more insights are needed to be able to derive accurate mathematical models in shallow water. To identify and decompose the effects of shallow water on a sailing ship, three model test campaigns were performed over the last two years with the 110m MARIN Inland Standard Ship (MISS 110), a representative class-Va inland ship (Bedos, 2019, 2020, 2021).
This investigation was mainly carried out in the Offshore Basin at MARIN. Thanks to its large dimensions and movable concrete floor, it combines the advantages of

model testing (controlled environment, adjustable water depth) without introducing undesirable confined-water effects of traditional tanks.
Experiments were conducted in a captive set-up, at various water depths. All kinds of planar motions were imposed, using a Computerised Planar Motion Carriage (CPMC) technique. In particular, this enabled high-quality measurement during steady rotation motions, which cannot be performed in narrow tanks.
Additional stationary tests were executed in the narrower Shallow-Water Basin, also at MARIN. Results under various configurations bring insights on blockage effect, accuracy of measurement and repeatability.

The current paper presents these experiments in shallow water, and summarises the main findings.

2 TEST CASE

The investigation considered the 110m MARIN Inland Standard Ship (MISS 110) as test case. This open access hull is aimed to be used as a benchmark case. The experiments were carried out with MARIN model No. 9359, manufactured from wood at a linear scale ratio of 1:18. Figure 1 shows a picture of the ship model.

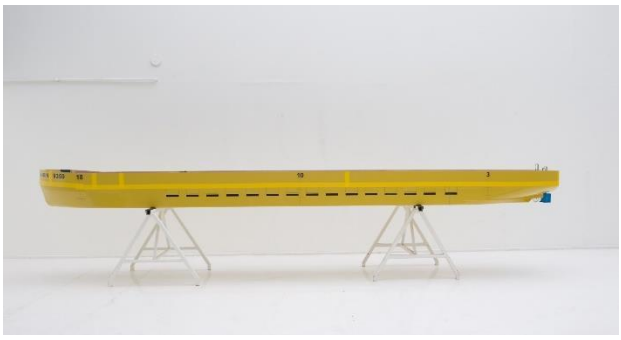

Figure 1. Scale model of MISS 110.

The ship was studied in full-load condition, corresponding to an even-keel draught of 3.50 m. Table 1 introduces its main particulars at rest, both at model and ship scales.

Table 1. Main particulars at rest.

Dimension	Unit	Model	Ship
Length overall	[m]	6.111	110.0
Breadth on waterline	[m]	0.633	11.4
Mean draught (even keel)	[m]	0.194	3.50
Displacement volume	[m^3]	0.665	3877
Block coefficient	[-]	0.883	0.883

The ship is fitted with a single ducted propeller and twin fishtail rudders with end-plates. The propeller measures 1.0 m in diameter and rotates clockwise. It is housed in a 19A-type nozzle. Table 2 and Table 3 provide further details about the ducted propeller and the rudders.

Table 2. Propulsion details.

Dimension	Unit	Model	Ship
Number of propellers	[-]	1	1
Nozzle type	[-]	19A	19A
Propeller diameter	[m]	0.100	1.80
Pitch ratio at 70% of radius	[-]	1.00	1.00
Number of blades	[-]	4	4
Direction of rotation	[-]	clockwise	

Table 3. Rudder details.

Dimension	Unit	Model	Ship
Number of rudders	[-]	2	2
Rudder type	[-]	fishtail	
Height	[m]	0.108	1.95
Chord	[m]	0.100	1.80
Lateral area (per rudder)	[m^2]	0.011	3.51

The two rudders are positioned at an offset of 0.80 m from the centreline. They feature large end-plates at the tip and root, and an asymmetric fishtail-type trailing edge. More details about the propulsion and steering arrangement can be found in Figure 2.

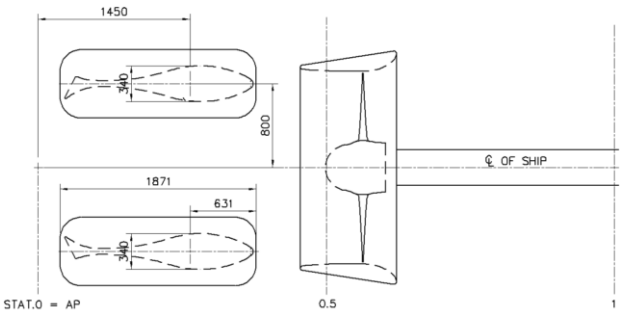

Figure 2. Propulsion and steering arrangement.

3 EXPERIMENTAL APPROACH

Three captive model test campaigns were performed at MARIN between June 2020 and November 2021. Such tests designate the measurement of a ship's hydrodynamic loads under a large range of imposed motions in a fully-controlled environment. The ship model was fixed to the moving carriage of one of MARIN's large basins, which imposed pre-defined motions and actuator controls. Thanks to a semi-captive set-up, the ship model could heave and pitch freely, while restricting the other four degrees. Thus, the model would experience dynamic squat the same way the full-scale ship would when sailing in shallow water (apart from scale effects, if any). While the carriage pulled the ship model along a given track, the manoeuvring loads applied to the ship and its actuators were recorded.

Most of the results presented here are extracted from experiments carried out in the Offshore Basin, which measures 45 m x 36 m in length and width. This basin is equipped with a movable concrete floor, enabling to adjust the water depth between 0 and 10 m (model scale). The

large dimensions of the basin minimise undesirable interactions that appear in shallow water, such as bank effect and residual current, making it possible to perform measurements in quasi-*unrestricted* shallow water. Figure 3 shows a photograph of the Offshore Basin during the tests with the MISS 110.

The Offshore Basin features a Computerised Planar Motion Carriage (CPMC) that can travel in longitudinal and transverse directions over the whole basin area. Thanks to its turn-table, the carriage can also apply rotations in yaw. Pre-defined tracks can therefore impose any combinations of surge, sway, yaw, propeller revolution and rudder angle, including non-stationary tests where one or more parameter is varying in a quasi-steady way (Hallmann, Quadvlieg, 2015).

Figure 3. Offshore Basin at MARIN.

In the Offshore Basin, tests were carried out with a fully-appended model (hull, propeller, nozzle, and rudders), at a water depth-to-draught ratio of h/T = 1.4 and 2.0 and various speeds. The test types included:

- **Load-variation tests:** propeller revolutions are varied with a constant longitudinal speed,
- **Static and non-stationary drift tests:** drift angle is kept constant or varied,
- **Static and non-stationary rotation tests:** yaw rate is kept constant or varied, with a longitudinal speed or at rest,
- **Static and non-stationary combined drift and rotation tests:** yaw rate is varied, with a constant drift angle,
- **Rudder sweep tests:** rudder angle is varied, at various propeller loading, and with or without a drift angle and/or yaw rate,
- **Oscillation tests:** whole model oscillates in surge, sway, or yaw.

Figure 4 proposes an example of motion track imposed to the ship model in the Offshore Basin. It shows a rotation test at constant yaw rate. The green grid represents markings on the concrete floor.

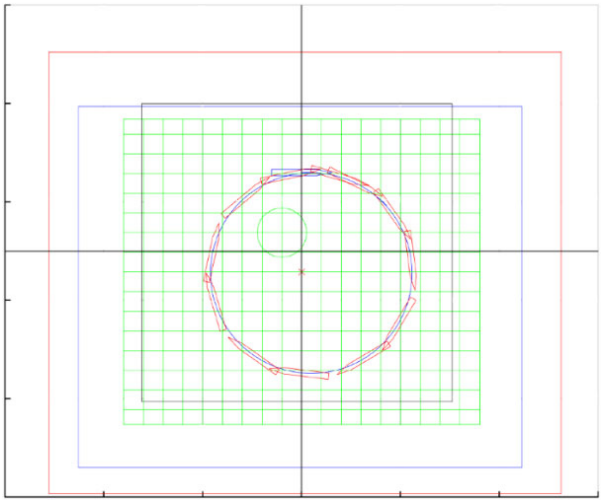

Figure 4. Example of track for static rotation test.

Additional experiments were carried out in the Shallow-Water Basin, which measures 220 m x 15.8 m in length and width. This basin features a fixed concrete floor and a set of pumps to adjust the water depth between 0 and 1.1 m (model scale). Because of its limited width, blockage effects are more likely to occur during experiments. Figure 5 shows a view of the carriage from one end of the basin.

Figure 5. Shallow-Water Basin at MARIN.

Like conventional tanks, the Shallow-Water Basin features a carriage travelling in the longitudinal direction of the basin only. The ship model was mounted in a fixed position, without a turn-table or a Planar Motion Mechanism (PMM). The set-up allowed stationary surge and sway motions, as well as any dynamic variations of propeller revolution and rudder angle. Rotation motions were not allowed by this set-up.

In the Shallow-Water Basin, the test types included:

- Load-variation tests,
- Static drift tests,
- Rudder sweep tests.

Experiments were carried out both with a bare-hull and fully-appended model, at a water depth-to-draught ratio of h/T = 1.2, 1.4 and 2.0. Several speeds were also considered.

4 RESULTS

The results presented here focus on the hull forces. More details about loads on appendages and interaction effects can be requested on demand.

4.1 PRELIMINARY CONSIDERATIONS

Hull forces and ship motions are given in a right-handed, ship-fixed direct coordinate system (see Figure 6). The origin is located at the intersection of the midship section, centreline, and waterline at rest.

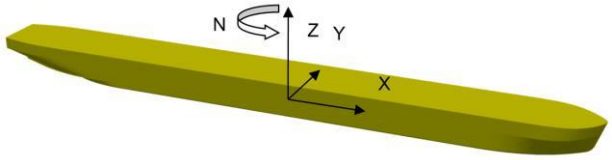

Figure 6. Ship-fixed coordinate system.

With the ship moving in the horizontal plane only, its velocity has longitudinal and transverse components u and v, and a rotation component in the horizontal plane r. To be closer to common nautical quantities, the ship motions are described as a function of total ship velocity V_s, drift angle β and non-dimensional rate of turn r', defined as:

$$V_s = \sqrt{u^2 + v^2} \tag{1}$$

$$\beta = \operatorname{atan}\left(\frac{v}{u}\right) \tag{2}$$

$$r' = \frac{r \cdot L_{PP}}{V_s} \tag{3}$$

To compare tests at different speeds, the hull forces and moment X, Y, N are expressed in a non-dimensional fashion, using the ship speed V_s, the water density ρ, and the ship's mean draught T.

$$X' = \frac{X}{0.5 \cdot \rho \cdot L_{PP} \cdot T \cdot {V_s}^2} \tag{4}$$

$$Y' = \frac{Y}{0.5 \cdot \rho \cdot L_{PP} \cdot T \cdot {V_s}^2} \tag{5}$$

$$N' = \frac{N}{0.5 \cdot \rho \cdot {L_{PP}}^2 \cdot T \cdot {V_s}^2} \tag{6}$$

In this section, the following tags are used to refer to the different test configurations:

- **[OB APP]** refers to tests conducted in the Offshore Basin with an appended model. Most tests were done at a speed of 12 km/h. Only tests with drift angles larger than 15 deg were performed at a lower speed, namely 4 km/h.
- **[BT APP]** refers to tests conducted in the Shallow-Water Basin with an appended model. All tests were carried out at a speed of 12 km/h.
- **[BT BH]** refers to tests conducted in the Shallow-Water Basin with a bare-hull model. Most tests were done at a speed of 12 km/h. Only tests with drift angles higher than 15 deg were performed at a lower speed, namely 4 km/h.

For all appended tests, propeller revolutions were set to model self-propulsion point when sailing straight at 12 km/h. For tests under large drift angles (at a speed of 4 km/h), revolutions were set to 0 rpm. Full-scale speeds of 12 and 4 km/h correspond to model-scale values of 0.786 and 0.262 m/s respectively.

Although some tests were realised with an appended model, the contributions of the propeller, duct, rudders and their interactions were subtracted to be able to compare *hull* forces in the next sections. The main advantage of using an appended model is that it is a realistic configuration. At higher speeds, results will include propeller-hull interactions due to propeller suction in the aft-body. Additionally, the ship will experience a different trim and sinkage due to this propeller section, which lead to variations in hull forces between a bare-hull and appended configuration.

In the figures shown in the next sections, [OB APP] results are represented with full lines, [BT APP] with dashed lines, and [BT BH] with dotted lines. Tests performed at a water depth-to-draught ratio of h/T = 2.0, 1.4 and 1.2 are plotted in blue, orange and grey colour respectively.

4.2 HULL LOADS UNDER SMALL DRIFT MOTIONS

Figure 7 and Figure 8 present the non-dimensional sway force Y' and yaw moment N' measured during experiments under small drift angles at a sailing speed of V_s = 12 km/h, with a fully-appended model.

A first effect of sailing in shallow-water can be identified in the increasing sway force and yaw moment when the water level reduces. Qualitatively, the relative difference in the sway force between h/T = 1.4 and 1.2 is at least equal to the difference between h/T = 2.0 and 1.4, and increases with β. This stresses the increasing influence of the hard bottom when distance with the keel becomes lower.

In medium deep water (h/T = 2.0), no significant difference appears between hull forces measured in the Offshore Basin and the Shallow-Water Basin. Nevertheless, they strongly appear at h/T = 1.4, where [BT APP] measurements consistently exceed [OB APP] measurements in the range of drift angles $\beta \in$ [-10, 0] deg. This exceedance averages 16% for Y' and N' at h/T = 1.4, while it is lower than 2% at h/T = 2.0.

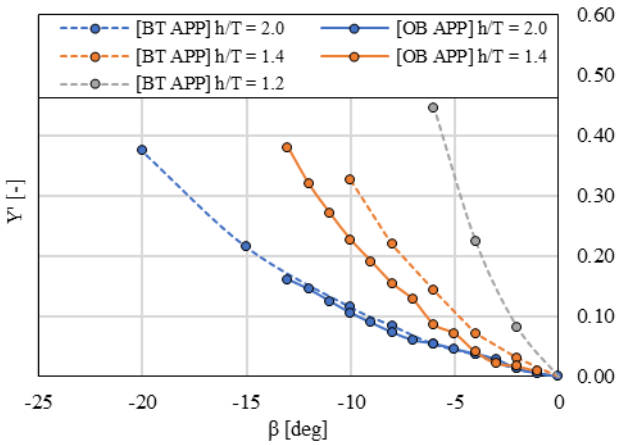

Figure 7. Experimental sway force under small drift motions at 12 km/h.

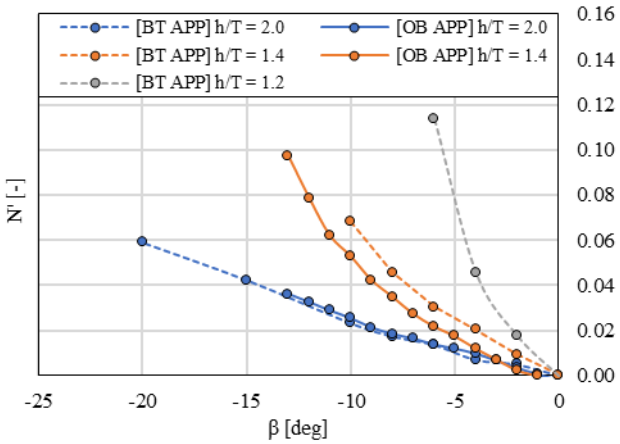

Figure 8. Experimental yaw moment under small drift motions.

The cross-section blockage in the Shallow-Water Basin, consequence of its narrower width, may explain such differences with experiments in the Offshore Basin, more than two times wider. The blockage factor is a measure of the space taken by a ship sailing in the cross-section of a canal or river. It is defined as the ratio between the immersed cross-section area of the ship and the cross-section area of the canal or river. The higher the blockage, the lower the space for the water to pass the ship, the stronger the interactions with the canal bottom and banks. Here, the ship cross-section is projected to the plane normal to the ship speed, to take the drift angle into account. To illustrate the difference in width between the Offshore Basin and the Shallow-Water Basin, Table 4 shows the blockage factors during the experiments in both facilities, for a run under a drift angle of 10 deg.

Table 4. Blockage factor during experiments, during test at 10 deg drift angle.

Facility	Unit	h/T		
-	[-]	2.0	1.4	1.2
Offshore Basin	[-]	0.02	0.03	
Shallow-Water Basin	[-]	0.05	0.08	0.09

4.3 HULL LOADS UNDER LARGE DRIFT MOTIONS

Figure 9 and Figure 10 present the hull non-dimensional sway force Y' and yaw moment N' measured during experiments under a large range of drift angles. The red vertical line at β = -15 deg is a marker of the change in ship speed. To remain close to realistic conditions, tests at low drift angles were carried out at V_s = 12 km/h, and the rest of the tests were done at V_s = 4 km/h, since at high drift angles the ship speed reduces.

The increase in hull forces and moments as the water level reduces, identified at low drift angles and higher speed, is also perceptible at larger drift angles. Thus, the relation $Y'(h/T = 1.2) > Y'(h/T = 1.4) > Y'(h/T = 2.0)$ is verified for the whole range of β. This is less obvious for the yaw moment at large drift angles, as N' decreases to very low values at β = -90 deg, consequence of its similar fore- and aft-bodies.

The non-dimensional form of hull sway force and yaw moment highlights a fairly large speed dependence. In deep water, it is often assumed that at reasonably-low speeds, hull forces vary linearly with V_s^2. This means that plotting non-dimensional forces as defined in Section 4.1 for tests performed at two different speeds would essentially result in a single line. The present tests evidence that this hypothesis does not stand in shallow water, even at Froude numbers as low as F_r = 0.10 and F_r = 0.03.

Indeed, a strong non-linearity is noticed at β = -15 deg, between tests at 12 km/h and 4 km/h. This is especially remarkable for the yaw moment at h/T = 1.2, but it is also clearly tangible at h/T = 1.4.

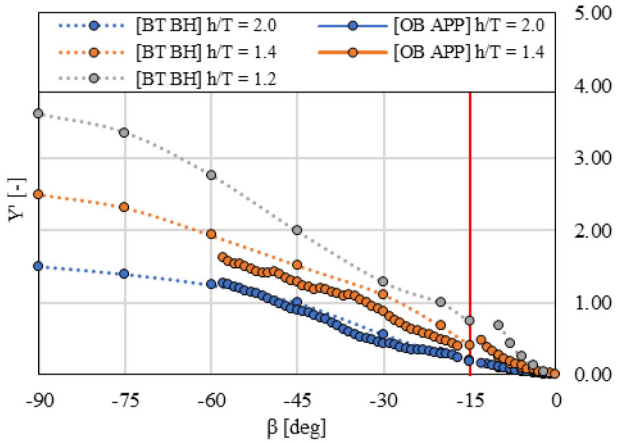

Figure 9. Experimental sway force under large drift motions.

The dynamic trim and sinkage of the ship in shallow water explains such speed dependence. Water pushed away by a ship sailing in shallow water cannot escape downward as it would in deep water. Consequently, it is sucked under

the keel, creating a low-pressure area pulling the ship down and known as squat effect. At higher speeds, the flow velocity under the keel increases, enhancing the dynamic sinkage (and trim) experience by the ship. For this reason, sailing at two different speeds in shallow-water conditions results in different under-water bodies, even at low Froude numbers. An example is the case β = -15 deg for [BT BH] at h/T = 1.4. At a speed of 4 km/h, the ship experiences a dynamic sinkage of 0.3% of its draught at rest T. At a speed of 12 km/h, the sinkage raises up to 5.5% of T.

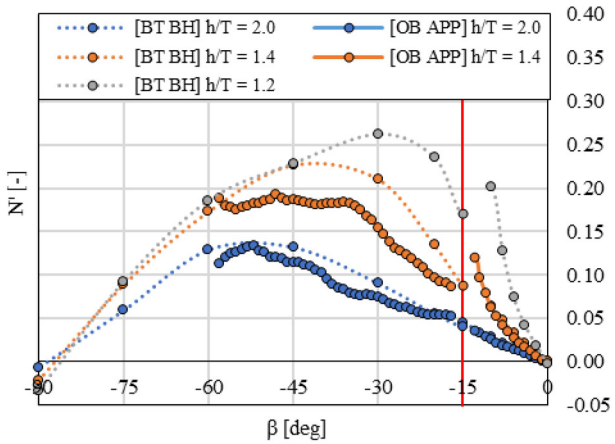

Figure 10. Experimental yaw moment under large drift motions.

Figure 9 and Figure 10 also evidence that, at h/T = 1.4, the sway force and yaw moment measured in the Offshore Basin are lower than in the Shallow-Water Basin in the range of drift angles $\beta \in$ [-60, -15] deg. In deeper water (h/T = 2.0), this difference is smaller, in particular for Y'. The immersed cross-section of the ship drastically increases at large drift angles, as the model length occupies a large part of the basin width. At a drift angle of 90 deg and a water depth-to-draught ratio of h/T = 1.4, the blockage factor reaches 28% in the Shallow-Water Basin. With such values, large interactions can be expected between the hull and the walls in this basin. Table 5 shows the experimental sway force during tests under 90 deg drift angle in both basins. In mild shallow water, [BT BH] results exceed [OB APP] by 9%. This greatly increases at h/T = 1.4, where it raises up to 38%.

Table 5. Experimental hull sway force Y' under 90deg drift angle.

Basin entry	Unit	h/T		
-	[-]	2.0	1.4	1.2
[OB APP]	[-]	1.37	1.81	
[BT BH]	[-]	1.50	2.50	3.60

A small part of the discrepancies between [OB APP] and [BT BH] may be explained by the difference in configuration. Although only hull forces are shown, tests in the Offshore Basin were conducted with an appended model, while [BT BH] experiments were carried out with the bare hull. This difference in set-up remains with minor impact, as the low test speed of 4 km/h and the propeller revolution of n = 0 rpm involve limited interactions.

4.4 HULL LOADS UNDER ROTATION MOTIONS

Thanks to its large width and its CPMC functionality, the Offshore Basin enables stationary and non-stationary runs under rotation motion. An example was shown in Figure 4, where a steady rotation rate of r' = 0.60 was imposed to the ship while sailing at a speed of 12 km/h, for a total test duration of more than 3 min (model scale). This corresponded to a yaw rate of roughly 62 deg/min.

Figure 11 and Figure 12 present experimental hull forces under rotation motions. These tests were performed at various drift angles to investigate the hydrodynamic loads under combined drift and rotation motions. Runs at β = 0, -6 and -15 deg are identified by circle, triangle and diamond markers respectively.

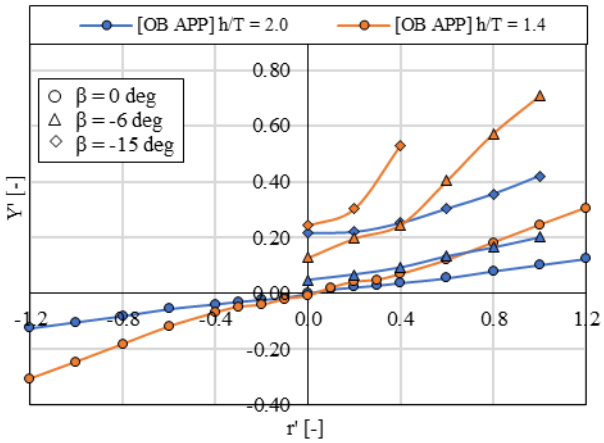

Figure 11. Experimental sway force under rotation motions.

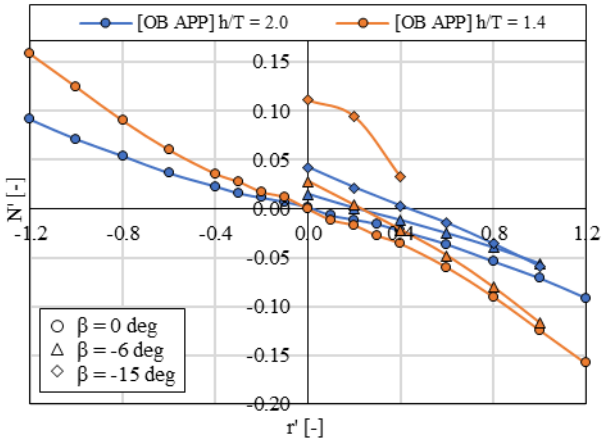

Figure 12. Experimental yaw moment under rotation motions.

Manoeuvring loads of a ship under rotation motions are highly influenced by the water level, in a similar fashion as they were shown to be under drift motions. This influence is also noticeable for combined motions.

It is important to point out that the magnitude of the hydrodynamic loads (*Y'* and *N'*) under rotation motions are significantly lower than *Y'* and *N'* induced by drift motions only.
Experimental data presented here provides valuable validation material for numerical predictions. It can be further used to determine a mathematical model for time-domain simulations or to compare to predictions using other methods, such as CFD computations. More details can be provided upon request.

4.5 SQUAT IN OFF-DESIGN CONDITION

As mentioned previously, the semi-captive set-up enabled the ship to freely heave and pitch as a result of sailing in shallow water. Due to the time required to reach an equilibrium at speed and the low magnitude of dynamic trim and sinkage, motions recorded in long stationary runs show a better accuracy. Consequently, this section presents results of experiments carried out in the Shallow-Water Basin, making full use of its length.
Figure 13 and Figure 14 present experimental dynamic sinkage and trim under small drift motions while sailing at a speed of 12 km/h. Squat motions were recorded by means of camera motion capture.

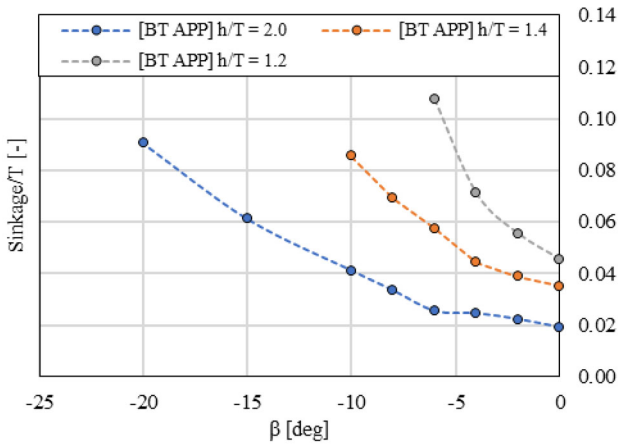

Figure 13. Experimental dynamic sinkage under small drift motions at 12 km/h.

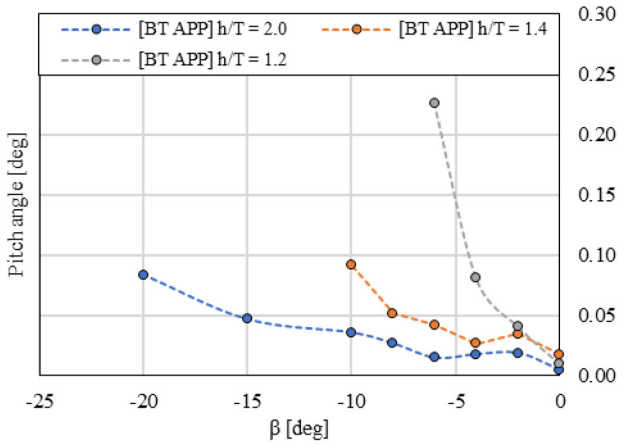

Figure 14. Experimental dynamic pitch angle under small drift motions at 12 km/h.

Measurements show a considerable effect of the drift angle and water depth on the dynamic trim and sinkage of the ship. As mentioned in Section 4.3, both motions drastically increase as the water level gets lower.
At β = 0 deg and h/T = 2.0, the dynamic sinkage equals 2% of the ship draught T. It increases to 3.5% at h/T = 1.4 and 4.5% at h/T = 1.2.
Under drift motions, the ship sinks to higher and higher values, reaching more than 10 %T for β = -6 deg and h/T = 1.2, which corresponds to half of the under-keel clearance at rest

The dynamic trim of the appended ship appears positive in all conditions presented in Figure 14, meaning that the bow goes down. It has sensibly the same sensitivity to drift angle and water depth as the dynamic sinkage. At a water depth-to-draught ratio of 2.0 and 1.4 and a drift angle of -6 deg, the pitch angle does not exceed 0.05 deg, which corresponds to an elevation difference of 10 cm between the bow and the stern. This elevation difference goes up to 44 cm (or 12.6% of the mean draught at rest) in the case at h/T = 1.2.

With dynamic sinkage, the overall submerged volume increases, which will have a direct effect on hull forces, and in particular *Y'*. Besides, the dynamic sinkage, here bow down, create an imbalance between fore and aft submerged hull volume, highly influencing *N'*.

The significant squat experienced by the ship in off-design conditions confirms the importance of accounting for this effect in numerical predictions. Without it, large discrepancies in hydrodynamic loads can be expected. Classical empirical formulas cannot be used because they only consider the ship sailing in straight motion. Various solution exist, such as a direct resolution of these 2 degrees of freedom in CFD calculations (Oud, Toxopeus, 2022).

5 CONCLUSIONS

An extensive experimental investigation, carried out in three different campaigns and in two different basins, over the manoeuvring forces of the 110m MARIN Inland Standard Ship (MISS 110) in shallow water was presented. It brings valuable validation material for numerical predictions of manoeuvring loads and motions. In particular, this set of data includes hull forces and moments under stationary and non-stationary rotation motions under low blockage factor, thanks to MARIN's wide Offshore Basin.
The study makes experimental data available to the public. It also evidenced the increase in hull loads for lower under-keel clearances and the effect of blockage on experimental results in conventional tanks. It also showed the non-linearity of hull loads with respect to V_s^2 in very shallow water, and linked it to the squat effect.

6 REFERENCES

Bedos, A., 2019. Inland Ship (110 m): Manoeuvring Model Tests in Shallow Water. MARIN Report No. 30957-2-BT.

Bedos, A., 2020. Inland Ship (110 m): Manoeuvring Model Tests in Shallow Water – Year 2020. MARIN Report No. 30957-6-BT.

Bedos, A. 2021. Inland Ship (110 m): Captive Manoeuvring Model Tests in Shallow Water in the Offshore Basin. MARIN Report No. 80414-1-OB.

Hallmann, R., Quadvlieg, R., 2015. Instationary Captive Model Tests, in: International Conference on Ship Manoeuvrability and Maritime Simulation (MARSIM), Newcastle, UK.

Mucha, P., Dettmann, T., Ferrari, V., El Moctar, O., 2019. Experimental investigation of free-running ship manoeuvers under extreme shallow water conditions. Appl. Ocean Res. 83, 155–162. https://doi.org/10.1016/j.apor.2018.09.008

Oud, G., Toxopeus, S., 2022. A Technique for Efficient Computation of Steady Yaw Manoeuvres Using CFD. To be published in: International Shipbuilding Progress.

Raven, H.C., 2019. A method to correct shallow-water model tests for tank wall effects. J. Mar. Sci. Technol. 24, 437–453. https://doi.org/10.1007/S00773-018-0563-1

Raven, H.C., 2019. Shallow-Water Effects in Ship Model Testing and at Full Scale, in: 5th MASHCON conference, Oostende, Belgium, pp. 341-352.

7 AUTHORS BIOGRAPHY

Antoine Bedos holds the position of Project Manager at MARIN in the Netherlands. He is conducting experimental and numerical research for the maritime industry, with a focus on shallow-water and manoeuvring applications. Over the past few years, he has conducted a large amount of model tests in shallow water for various contractual and fundamental research projects. He is also expert in mathematical manoeuvring models and time-domain simulations.

Roberto Tonelli holds the position of Senior Researcher at MARIN in the Netherlands. He is also Coordinator of the research programme *Manoeuvring & Nautical studies*.